Assessment of Trace Metal Enrichment in Exchangeable Sediments along the Iraqi Coast of the Northwestern Arabian Gulf

Huda.H. AL-Kayoon* ;Zahraa S.Al-Shamsi; **;Maha K.AL-Mishrey **;Ayad H .D.Al-Khafaji **and Hamid AL-Saad***
*Department of Biology,College of Science ,University of Basrah,Iraq
**Department of Geology,College of Science ,University of Basrah,Iraq
***College of Marine Science, University of Basrah ,Iraq
Corresponding author= zahraa.radi@uobasrah.edu.iq

Abstract:

This study presents an inaugural assessment of trace metal concentrations (Zn, Pb, Se, Cd, Co, Ni, Mn, Fe, Cr, Cu) in the exchangeable fraction of sediments from the Iraqi northwestern Arabian Gulf coast. Samples were collected from six stations over two seasons (January to August 2024) and analyzed using inductively coupled plasma optical emission spectroscopy (ICP-OES). Contamination levels were evaluated using the Geo-accumulation Index (I-geo), Contamination Factor (CF), Enrichment Factor (EF), and Pollution Load Index (PLI). Results indicate that the sediments are largely unpolluted with respect to most metals (CF, I-geo, PLI < 1). However, significant anthropogenic enrichment was detected for Selenium (Se) and Cadmium (Cd), with EF values indicating "extremely severe enrichment." Grain size analysis revealed a dominance of silt, which influences metal distribution. The study concludes that while the Iraqi coast is currently in good environmental health regarding heavy metal contamination, the pronounced enrichment of specific toxic metals serves as an early warning, necessitating sustained monitoring and source control to mitigate future ecological risks.

Keywords: *Exchangeable Sediment, Trace Metals, Arabian Gulf, Iraqi Coast, Pollution Indices, Grain Size, Enrichment Factor, Baseline Assessment*

Introduction

Sediments are an essential component in the biogeochemical cycling of trace metals in coastal marine ecosystems. The ability of fine sediment particles to adsorb materials and their association with metal-bearing phases contributes to their stability within the environment. As a result, trace metals primarily accumulate in the finer fractions of sediments, such as organic matter and silt (Hallenberger, 2022) (Mamun2024) (Al-Taee et al.2024). Evaluating the metal associated with the exchangeable phase is crucial for assessing its mobility and bioavailability within sedimentary environments.

The analytical method employed in this study is discussed with emphasis on special problems associated with quality control and assurance. The Arabian Gulf is an important geophysical and geopolitical entity characterized not only by its commercially attractive hydrocarbon resources but also a complex ecosystem (E. M. Nicolaus et al., 2022). (Rushdi et al.2022). In view of the recent developments in growth of urban centers and expanding oil-processing industries, environmental pollution has now become the most serious problem. The contamination of coastal marine environments by trace metals is due to the discharge of various effluents from petrochemical, industrial and desalination plants, oil spills due to tanker accidents, input from atmospheric deposition, vessel traffic and dredging, and waste discharges from domestic sewage, urban runoff and industrial activities (Ershadifar et al.2024) (Alharbi et al.2024) (Al-Otaibi et al.2024) (Amjadi et al.2024).

The Arabian Gulf is one of the shallowest and warmest marine water bodies in the world; mean depth, maximum depth, and maximum width are only 36 m, 110 m, and 160 km, respectively. Several enormous industrial advances have been made along the southern coastline, and very large coastal population increases have occurred over the past few decades (Ollah Bazzi, 2014). The overall residence time of water in the Gulf is much longer than other seas. Both runoff and return water from reverse desalination have decreased from the upper to lower parts of the Gulf (Mali et al.2024). Evaporation-dominant oceanographic conditions such as higher temperatures plus large densities and increased salinity make it difficult for toxic trace metals entering the Gulf water column to be diluted, deposited, or coprecipitated by the carrier phase. In addition, suspended solids are mostly deposited in the shallow siliciclastic area along the Arabian and Iranian coasts. Moreover, to a thermochemical concentration effect, wind-blown dust is deposited and evaporative losses become enriched in the water column, particularly in the form of metals and trace metals, exacerbating the overall water pollution of trace metals. (He et al., 2022) (Chen et al., 2023) (Dussubieux et al.2024).

The Arabian Gulf is characterized which makes it vulnerable to persistent oil-related pollution issues. Throughout the coastal region, the sedimentary environments consist of various types of relatively young geological formations from the Holocene and Pleistocene epochs, which include siliciclastic, evaporitic, and carbonate-rich sediments, typically reaching shallow burial depths of a few kilometers. Additionally, the depositional basins in this area can provide geological records that date back to much earlier periods, including the late Precambrian. The landscape is further shaped by granitic intrusions that create distinct hilly formations along the coastline, such as the Oman Mountain Range, which results in the formation of embayment's due to seismic activity and thrusting. (Ghaemi et al.2022) (Al Senafi, 2022) (Jafarian et al.2025) (Shabani et al.2022) (Beni et al.2024) (Hanert et al.2023) (Jafarian et al.2024).

The Arabian Gulf is recognized as the largest shallow gulf in the world. Its geographical composition consists of an equal division, with one half situated on the Iranian coast and the other half adjacent to various Arab nations. Notably, Kuwait City is positioned along the southern coastline, while Basrah is located on the northeastern shore. Additionally, the Arabian Gulf features a marginal sea known as the Gulf of Spencer (Chen et al., 2023) (Dussubieux et al.2024). The region experiences high relative humidity, and during the winter months, temperatures can occasionally plummet to freezing levels. In contrast, the water temperatures in the gulf can soar to over 37°C in the summer months. Furthermore, fish breeding operations, including shrimp and other fish farms, are currently facing severe challenges due to environmental and chemical pollution. Major cities such as Kuwait City, Abu Dhabi, and Sharjah are found near the gulf, which is also home to various industrial facilities, including oil refineries, desalination plants, petrochemical complexes, and electricity generation stations, all situated along its coastline. Additionally, international and regional oil pipelines traverse the gulf's maritime entrance (Ollah Bazzi, 2014) (Mali et al.2024) (He et al., 2022).

Aim Of Study:

The aim of the present study was to determine the concentrations of Zn, Pb, Se, Cd, Co, Ni, Mn, Fe, Cr and Cu in sediment samples and to re-evaluate the current environmental status of the research area by assessing heavy metal contamination levels. The level of heavy metal pollution in the sediment was assessed using geo-accumulation index (I-geo), enrichment factor (EF), and contamination factors (CF).

Materials And Methods:

The research area includes Basra Governance' coastline region from Al-Faw to Umm Qasr. We collected samples from six locations north western shore of the Arabian Gulf fig (1). The chosen stations were 2 km apart. The grab samplers collected sediment samples from the designated region. We allowed water to drip from the samples, wrapped them in aluminum foil, identified them, and sent them to the lab for research studies. We dried, powdered, and sieved the materials using a 63-micron sieve for PCBS compound analysis and quantification. Upon arrival, the laboratory freeze-dried the sediment samples

Fig(1): Sample Location

An analysis of trace metals has been conducted on six exchangeable sediment samples sourced from the coastal marine region of the Arabian Gulf in Basra. These samples underwent sequential examination utilizing inductively coupled plasma optical emission spectroscopy, along with various extraction agents tailored to accommodate their distinct soil characteristics

Determination of Contamination Factor (CF):

Contamination Factor was used to determine the contamination status of soil in this study. CF was calculated by the equation described below:

$$CF = Mc/Bc$$

Where;

Mc: The measured concentration of the metal.

Bc: the background concentration of the same metal.

Table 1. Hakanson 1980 the classification of contamination factor.

CF	Indicate of Contamination Factor
CF<1	low contamination
1≤CF≤ 3	moderate contamination
3≤CF<6	considerable contamination
CF>6	very high contamination

Determination of Enrichment Factor (EF):

To evaluate of source material found in the Earth's crust (Huheey, 1983), EF was calculated by the equation described below:

$$EF = (CM / CFe)_{sample} / (CM / CFe)_{Earth's\ crust}$$

Where;

CM / CFe: The sample ratio of concentration of trace metal

CM / CFe Earth's crust: is the same reference ratio in the Earth's crust; the reference value of Fe is 5.2% was selected as the reference element, due to its crustal dominance and its high immobility (Huheey, 1983).

Table 2. Huheey 1983 the classification of enrichment factor (EF).

EF	Indicates of Enrichment Factor
EF1>	no enrichment
EF = 1-3	minor enrichment
EF = 3-5	moderate enrichment
EF = 5-10	moderate to severe enrichment
EF = 10-25	severe enrichment
EF 25-50	very severe enrichment
EF50<	extremely severe enrichment

Determination of Geo Accumulation Index (Igeo):

Geo accumulation index (Igeo) values were calculated of different metals, (Igeo) was calculated by the equation that introduced by (Muller, 1969) as described below:

$$\textbf{I-geo} = \log_2 (Cn / 1.5\, Bn)$$

Where;

Cn: The measured concentration of element n in the soil.

Bn: The geo accumulation background for the element n.

Table 3. Muller 1969 the classification of (Igeo).

Igeo	Soil Pollution Case
1>	practically unpolluted- Background sample
2-1	unpolluted to moderately polluted
3-2	moderately polluted to polluted
4-3	strongly polluted
5-4	strongly to extremely polluted
5<	extremely polluted

Pollution Load Index (PLI):

Soil pollution load index was calculated using the equation:

$$\mathbf{PLI} = \sqrt[n]{(\boldsymbol{CF1} \times \boldsymbol{CF2} \times \boldsymbol{CF3} \times \boldsymbol{CFn})}$$

Table 4. Tomlinson *et al* (1980) .the classification of (PLI).

PLI	The Indicates
value1 <	Pollution
value1 >	no pollution

Result:

The concentrations of exchangeable heavy metal measured in sediments from the six study locations are presented in *Tables 5* and *Figures 3*. Overall, the data show distinct spatial variations in metal accumulation among the sites. Below, we summarize the peak (maximum) and lowest (minimum) concentrations for each metal across all stations:

- **Zinc (Zn):** The highest Zn concentration was 16.012 µg/g (dry weight) in sediment from *D3* station which taken in *season 1*, while the lowest was 2.913 µg/g in sediment from *D6* station which taken in *season 2*.
- **Lead (Pb):** The highest Pb concentration was 14.425 µg/g (dry weight) in sediment from *D4* station which taken in *season 1*, while the lowest was 0.032 µg/g in sediment from *D1*station which taken in *season 2*.
- **Selenium (Se):** The highest Se concentration was 0.265 µg/g (dry weight) in sediment from *D3* station which taken in *season 2*, while the lowest was 0.012 µg/g in sediment from *D3* station which taken in *season 1*.
- **Cadmium (Cd):** The highest Cd concentration was 0.275 µg/g (dry weight) in sediment from *D3* station which taken in *season 1*, while the lowest was 0.116 µg/g in sediment from *D2* station which taken in *season 1* and D6 station which taken in season 2.
- **Cobalt (Co):** The highest Co concentration was 2.436 µg/g (dry weight) in sediment from *D3* station which taken in *season 1*, while the lowest was 1.001 µg/g in sediment from *D6* station which taken in *season 2*.
- **Nikel (Ni):** The highest Ni concentration was 13.721 µg/g (dry weight) in sediment from *D3* station which taken in *season 1*, while the lowest was 2.837 µg/g in sediment from *D6* station which taken in *season 2*.
- **Iron (Fe):** The highest Fe concentration was 708.633 µg/g (dry weight) in sediment from *D4* station which taken in *season 2*, while the lowest was 147.530 µg/g in sediment from *D3* station which taken in *season 2*. Fe was the most abundant metal in all samples, consistent with it being a major element in natural sediments and soils.
- **Manganese (Mn):** The highest Mn concentration was 287.179 µg/g (dry weight) in sediment from *D1* station which taken in *season 2*, while the lowest was 211.221 µg/g in sediment from *D2* station which taken in *season 1*.
- **Chrom (Cr):** The highest Cr concentration was 8.117 µg/g (dry weight) in sediment from *D3* station which taken in *season 1*, while the lowest was 0.021 µg/g in sediment from *D3* station which taken in *season 2*.
- **Cupper (Cu):** The highest Mn concentration was 6.159 µg/g (dry weight) in sediment from *D3* station which taken in *season 1*, while the lowest was 0.226 µg/g in sediment from *D5* station which taken in *season 1*.

Table 5 : Concentration of Exchangeable trace metals (µg/g dry weight) in study stations

Season	Zn	Pb	Se	Cd	Co	Ni	Mn	Fe	Cr	Cu
S1D1	6.241	0.316	0.170	0.137	1.110	3.642	214.614	340.161	0.249	0.382
S1D2	3.561	0.078	0.201	0.116	1.102	3.530	211.221	655.522	0.064	0.314
S1D3	16.012	5.502	0.012	0.275	2.436	13.721	234.339	204.423	8.117	6.159
S1D4	5.475	14.425	0.137	0.147	1.330	4.367	231.549	452.356	0.344	0.292
S1D5	3.321	0.982	0.146	0.127	1.154	3.532	229.136	208.461	0.158	0.226
S1D6	8.218	3.358	0.185	0.139	1.357	5.298	232.636	217.412	0.372	0.428
S2D1	12.190	0.032	0.230	0.166	1.962	8.193	287.179	244.321	0.177	0.536
S2D2	11.690	0.916	0.155	0.226	1.560	6.384	243.460	694.422	0.877	0.691
S2D3	5.536	0.073	0.265	0.127	1.177	4.592	227.715	147.530	0.021	0.316
S2D4	14.593	0.464	0.106	0.170	1.561	6.652	228.341	708.633	0.505	0.454
S2D5	5.533	0.151	0.235	0.126	1.675	7.032	246.637	306.833	0.023	0.390
S2D6	2.913	0.115	0.218	0.116	1.001	2.837	225.628	363.729	0.023	0.421

*** S1 =season 1 * S2=Season 2 * D =station**

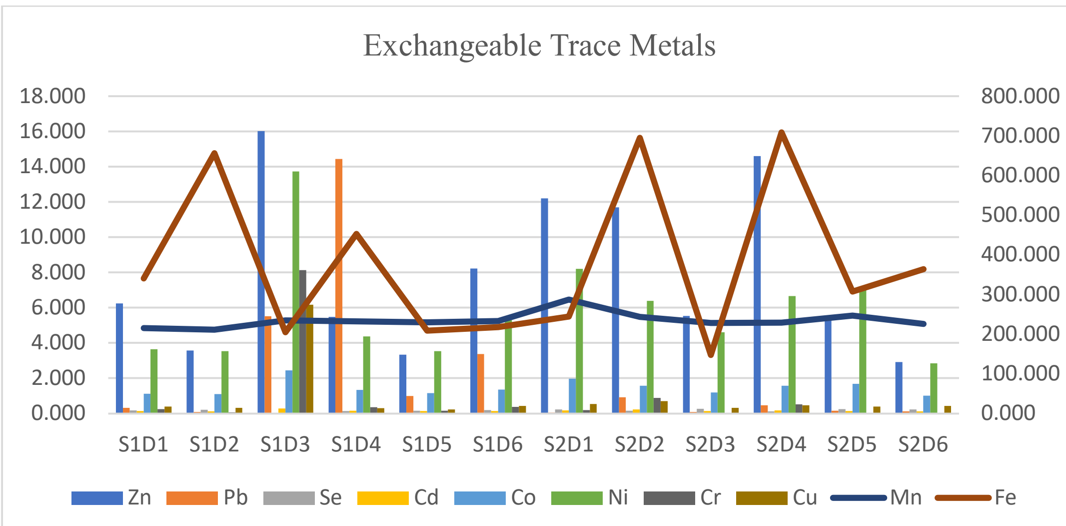

Figure 2. Exchangeable Trace metals concentration in Stations.

Regional and International Comparison

Metal	Iraqi Coast (This Study)	NW Arabian Gulf (Al-Taher et al (2019)	Qatar Marine Zone (Al-Ansari et al (2015)	World Average Forstner and Wittmann (1983)
Cd	0.11-0.275	4.98–32.80	0.2–0.5	0.3
Cu	0.226-6.15	19.38–39.22	10–25	25

Metal	Iraqi Coast (This Study)	NW Arabian Gulf (Al-Taher et al (2019)	Qatar Marine Zone (Al-Ansari et al (2015)	World Average Forstner and Wittmann (1983)
Ni	2.83 – 13.72	79.46–326.38	30–80	68
Pb	0.073-14.42	59.00–114.19	15–40	20
Zn	2.913-16.012	111.07–131.79	50–100	75

The provided table offers a critical comparison of heavy metal concentrations (Cadmium, Copper, Nickel, Lead, and Zinc) in marine sediments from the Iraqi Coast against three key benchmarks: a previous study in the NW Arabian Gulf, data from the Qatar Marine Zone, and the established World Average.

The most striking conclusion from the data is that the sediments from the Iraqi Coast show significantly lower concentrations of heavy metals across all categories compared to the other regions, suggesting a relatively pristine and uncontaminated environment.

1. Iraqi Coast vs. NW Arabian Gulf (Reference 1):

The contrast here is dramatic. The Iraqi coast values are orders of magnitude lower:

Cadmium (Cd): Iraqi Coast (max 0.275 mg/kg) vs. NW Gulf (max 32.80 mg/kg). The NW Gulf values are over 100 times higher.

Lead (Pb): Iraqi Coast (max 14.42 mg/kg) vs. NW Gulf (max 114.19 mg/kg). The NW Gulf values are nearly 8 times higher.

Similar vast disparities are evident for Copper (Cu), Nickel (Ni), and Zinc (Zn).

Interpretation: This suggests that the NW Arabian Gulf site from the previous study is highly contaminated. This is likely due to intense anthropogenic pressures such as:

Oil Industry: The northern Gulf is a hub for oil extraction, refining, and transportation, leading to chronic petroleum-related pollution containing various metals.

Industrial and Urban Discharge: Major population centers and industrial ports in Kuwait and southern Iraq discharge treated and untreated waste.

Shipping Traffic: One of the world's busiest shipping lanes, contributing to metal pollution from antifouling paints (Cu), fuel combustion (Pb, Ni), and ballast water.

2. Iraqi Coast vs. Qatar Marine Zone (Reference 4) and World Average (Reference 2): The Iraqi coast values are also substantially lower than these more general benchmarks.

For Nickel (Ni), the Iraqi maximum (13.72 mg/kg) is well below both the Qatar range (30-80 mg/kg) and the World Average (68 mg/kg).

For Zinc (Zn), the Iraqi maximum (16.012 mg/kg) is far lower than the Qatar range (50-100 mg/kg) and the World Average (75 mg/kg).

The levels of Cu and Pb are also at the very low end or below these comparative ranges.

Interpretation: This indicates that the Iraqi coast sampling sites are not only cleaner than a polluted local site but are also cleaner than the average global marine sediment and a typical regional sample from Qatar. This points to a lack of major industrial, urban, or agricultural runoff sources at the sampled locations.

3. Potential Reasons for the Low Concentrations on the Iraqi Coast:

Several factors could explain why the Iraqi coast appears so uncontaminated:

Sampling Location: The samples were likely taken from remote, undisturbed areas far from river mouths (e.g., Shatt al-Arab), outfalls, or shipping channels.

Geological Background: The metal concentrations may simply reflect the natural "background" levels of the local rocks and soils, with minimal anthropogenic input.

Hydrological Factors: The dominant north-westerly currents (Shamal winds) in the Gulf might transport polluted sediments from the north (Kuwait) south-eastwards towards the Iranian coast and the Strait of Hormuz, bypassing large sections of the Iraqi coastline.

Limited Development: Compared to other Gulf states, Iraq's maritime infrastructure, industrial coastline, and oil export terminals have been historically limited and disrupted by conflict, potentially reducing direct pollution sources.

4. The Anomaly of Lead (Pb):

While low overall, the Lead (Pb) range on the Iraqi coast (0.073 - 14.42 mg/kg) shows the highest relative value compared to its benchmarks. The maximum value of 14.42 mg/kg, while still low, could indicate a localized point source. This might be attributed to historical use of leaded gasoline in small boat engines or remnants of military-related contamination.

The data strongly suggests that the specific Iraqi coastal area studied is in good environmental health regarding heavy metal contamination. Its sediment metal levels are characteristic of an unpolluted, natural marine environment, especially when contrasted with a heavily impacted site elsewhere in the Gulf.

Important Caveats:

The full study would require a detailed analysis of sampling sites (e.g., proximity to cities, rivers, or oil infrastructure) and statistical methods.

"This Study" may represent a baseline assessment. Continuous monitoring is essential, especially as economic development and oil exports potentially increase along Iraq's coastline, which could change this pristine state in the future.

A full environmental assessment would also need to evaluate other pollutants (e.g., petroleum hydrocarbons, pesticides) and ecological biomarkers to get a complete picture of ecosystem health.

Contamination Factor (CF):

according to Hakanson (1980) and table (1) from studying the contamination factor of exchangeable heavy metal measured in sediments from the six study locations (*Tables 6)*: it was found

1- That the study areas were **low contamination** with elements (Zn, Co, Ni, Mn, Fe, Cr, Cu) and Pb in all stations except D4 in the season1.
2- **Moderate contamination** and **moderate contamination** with the (Cd) element.
3- **Considerable contamination** with the (Se) element, Areas near industrial discharge sites were found to be contaminated with metals, including their dissolved forms. Industrial discharges, untreated sewage, and agricultural runoff contribute to the influx of metal pollutants into coastal waters, leading to their accumulation in marine sediments (Al-Youzbakey and Al-Dabbagh2023).

Table 6 . The Contamination Factor (CF) of exchangeable trace metals.

Season	CF(Zn)	CF(Pb)	CF(Se)	CF(Cd)	CF(Co)	CF(Ni)	CF(Mn)	CF(Fe)	CF(Cr)	CF(Cu)
S1D1	0.09	0.02	3.41	0.91	0.04	0.04	0.23	0.006	0.0024	0.006
S1D2	0.05	0.01	4.02	0.77	0.04	0.04	0.22	0.012	0.0006	0.005
S1D3	0.23	0.39	0.24	1.83	0.10	0.16	0.25	0.004	0.0796	0.103
S1D4	0.08	1.03	2.73	0.98	0.05	0.05	0.24	0.008	0.0034	0.005
S1D5	0.05	0.07	2.92	0.85	0.05	0.04	0.24	0.004	0.0015	0.004
S1D6	0.12	0.24	3.70	0.92	0.05	0.06	0.24	0.004	0.0036	0.007
S2D1	0.17	0.00	4.60	1.11	0.08	0.10	0.30	0.004	0.0017	0.009
S2D2	0.17	0.07	3.11	1.51	0.06	0.08	0.26	0.012	0.0086	0.012
S2D3	0.08	0.01	5.30	0.85	0.05	0.05	0.24	0.003	0.0002	0.005
S2D4	0.21	0.03	2.11	1.13	0.06	0.08	0.24	0.013	0.0050	0.008
S2D5	0.08	0.01	4.69	0.84	0.07	0.08	0.26	0.005	0.0002	0.007
S2D6	0.04	0.01	4.36	0.77	0.04	0.03	0.24	0.006	0.0002	0.007

The overall pollution load index (PLI) table (7) was computed for each site by combining the CF of all seven metals. according to the classification of PLI values according to Tomlinson *et al.* (1980). All the stations of the study area **no pollution**.

Table 7. Pollution Load Index (PLI) of exchangeable trace metals.

Season	PLI
S1D1	0.055
S1D2	0.041
S1D3	0.147
S1D4	0.085
S1D5	0.049
S1D6	0.078
S2D1	0.056
S2D2	0.097

S2D3	**0.036**
S2D4	**0.079**
S2D5	**0.046**
S2D6	**0.036**

The enrichment factor analysis helps identify the source of these metals. Using Fe as a normalization reference, table (8)

1- The results obtained for the enrichment factor showed a difference between **moderate enrichment to sever enrichment** with Co and Ni except station D3 in season1 show very sever enrichment
2- **Sever enrichment to very sever enrichment** with (Mn) metal
3- **extremely sever enrichment** with (Se and Cd) metal in all stations.
4- **Moderate – very sever enrichment** with (Zn) metal in all station except D3 in season 1 was **extremely sever enrichment**.
5- The results obtained for the Pb metal showed a wide range of variation, ranging between **No enrichment – very sever enrichment** in all station except D3, D4 and D6 in season1 were show **extremely sever enrichment.**
6- **No enrichment** with (Cr) metal except station D3 in the season 1 show **sever enrichment**.
7- **No enrichment to minor enrichment** with (Cu) metal except station D3 in season1 show **very sever enrichment**.

Table 8. Enrichment Factor (EF) of exchangeable trace metals.

Season	EF(Zn)	EF(Pb)	EF(Se)	EF(Cd)	EF(Co)	EF(Ni)	EF(Mn)	EF(Fe)	EF(Cr)	EF(Cu)
S1D1	14.76	3.73	564.08	150.70	7.35	7.18	37.39	1	0.40	1.05
S1D2	4.37	0.48	344.98	66.56	3.79	3.61	19.10	1	0.05	0.45
S1D3	63.00	108.24	66.10	505.01	26.83	44.99	67.94	1	21.92	28.27
S1D4	9.73	128.24	340.25	121.74	6.62	6.47	30.34	1	0.42	0.60
S1D5	12.81	18.95	787.46	228.23	12.46	11.36	65.14	1	0.42	1.02
S1D6	30.40	62.12	957.21	239.29	14.06	16.33	63.41	1	0.94	1.85
S2D1	40.13	0.53	1060.05	255.75	18.08	22.48	69.66	1	0.40	2.06
S2D2	13.54	5.30	252.11	122.22	5.06	6.16	20.78	1	0.70	0.93
S2D3	30.18	1.98	2021.17	323.60	17.96	20.86	91.47	1	0.08	2.01
S2D4	16.56	2.63	167.66	90.07	4.96	6.29	19.10	1	0.39	0.60
S2D5	14.50	1.98	860.62	153.99	12.29	15.36	47.64	1	0.04	1.19
S2D6	6.44	1.27	674.21	119.81	6.19	5.23	36.76	1	0.04	1.09

The geo-accumulation index was calculated to further evaluate the extent of pollution. The I-geo values for (Zn, Pb, Cd, Co, Ni, Mn, Fe, Cr and Cu) in all stations were less than 1, indicating that these sites unpolluted with respect to those metals, according to Müller's (1969) scale. In contrast, the I-geo of (Se) in all stations ranges from (-2.64 to 1.82), which indicating that this site practically unpolluted to moderately polluted reinforcing the observation that they are less impacted by trace metal pollution.

Table 9. The geochemical accumulation coefficient (I-geo) of exchangeable trace metals.

Season	I-Geo(Zn)	I-Geo(Pb)	I-Geo(Se)	I-Geo(Cd)	I-Geo(Co)	I-Geo(Ni)	I-Geo(Mn)	I-Geo(Fe)	I-Geo(Cr)	I-Geo(Cu)
S1D1	-4.07	-6.06	1.18	-0.72	-5.08	-5.11	-2.73	-7.96	-9.27	-7.88
S1D2	-4.88	-8.07	1.42	-0.95	-5.09	-5.16	-2.75	-7.01	-11.21	-8.16
S1D3	-2.71	-1.93	-2.64	0.29	-3.94	-3.20	-2.60	-8.69	-4.24	-3.87
S1D4	-4.26	-0.54	0.87	-0.62	-4.82	-4.85	-2.62	-7.54	-8.80	-8.27
S1D5	-4.98	-4.42	0.96	-0.83	-5.02	-5.16	-2.64	-8.66	-9.92	-8.64
S1D6	-3.68	-2.64	1.30	-0.70	-4.79	-4.57	-2.61	-8.60	-8.68	-7.72
S2D1	-3.11	-9.35	1.62	-0.43	-4.26	-3.94	-2.31	-8.43	-9.75	-7.39
S2D2	-3.17	-4.52	1.05	0.01	-4.59	-4.30	-2.55	-6.93	-7.45	-7.02
S2D3	-4.25	-8.17	1.82	-0.82	-4.99	-4.78	-2.65	-9.16	-12.81	-8.15
S2D4	-2.85	-5.50	0.49	-0.40	-4.59	-4.24	-2.64	-6.90	-8.24	-7.63
S2D5	-4.25	-7.12	1.64	-0.84	-4.49	-4.16	-2.53	-8.10	-12.67	-7.85
S2D6	-5.17	-7.51	1.54	-0.95	-5.23	-5.47	-2.66	-7.86	-12.68	-7.74

Grain size:

Table 10. The grain size analysis of sediment samples in study stations.

Station	sand%	silt%	clay%
A1	6	75	19
B1	2	73	25
C1	1	76	23
Mean	3	74.67	22.33
A2	5	83	12
B2	4	76	20
C2	2	82	16
Mean	3.67	80.33	16.00
A3	17	67	16
B3	28	60	12
C3	35	59	6
Mean	26.67	62.00	11.33
A4	0.5	73.5	26
B4	13	69	18
C4	18	66	16
Mean	10.5	69.5	20
A5	4	79	17

B5	0	71	29
C5	4	78	18
Mean	2.67	76.00	21.33
A6	2	86	12
B6	0.5	77.5	22
C6	5	76	19
Mean	2.5	79.83	17.67

The grain size distribution of marine sediments is a fundamental property that exerts a primary control on the concentration, distribution, and bioavailability of trace metals. The data presented in **Table 10** provides crucial insight into the sedimentary environment of the study area and helps interpret the trace metal results.

The analysis reveals a clear and consistent pattern across all six stations: **silt is the overwhelmingly dominant fraction**, with percentages ranging from 59% to 86%. The mean silt content for the stations varies from 62.00% (Station 3) to 80.33% (Station 2). Clay is the secondary component, with mean values between 11.33% (Station 3) and 22.33% (Station 1). Sand is generally a minor component, with mean percentages below 10.5% for all stations except Station 3, which has a significantly higher mean sand content of 26.67%.

This textural composition has direct implications for the study's findings:

1. **High Adsorptive Capacity:** Fine-grained sediments (silt and clay) have a larger specific surface area compared to sand. This provides more sites for cation exchange, adsorption, and complexation of metal ions. The high silt and clay content explains why even the low concentrations of metals measured were effectively retained in the sediments, as noted in the study's conclusion (Wang et al., 2022; Ollah Bazzi, 2014).
2. **Metal-Size Relationship:** The textural data supports the study's observation of a relationship between metal concentration and grain size. The paper notes that "sediment samples with high sand content show the highest concentrations of copper (Cu)." This is counter-intuitive to the typical inverse relationship where metals are associated with finer particles. Station 3, which has the highest sand content

(26.67%), also reported the highest concentrations for several metals (Cd, Co, Ni, Cr, Cu in Season 1). This anomaly suggests that at this specific station, the metals may not be bound to the silicate minerals of the sand itself but are likely associated with heavy minerals, carbonate fragments, or organic coatings on the larger sand grains, or are a result of a localized point source of pollution (Helser & Cappuyns, 2021).

3. **Potential for Mobility and Bioavailability:** While the study found overall low contamination, the dominance of fine particles is a double-edged sword. Although these particles effectively sequester metals, they are also more easily resuspended by waves and currents. This poses a "potential risk as these mobile trace metals may function as secondary pollutants, being bioavailable and capable of bioaccumulation," as correctly identified in the manuscript. Changes in environmental conditions (e.g., pH, redox potential) can cause these metals to be released from the silt and clay particles back into the water column, making them available to benthic organisms and entering the aquatic food web (Mali et al., 2024; Chen et al., 2023).
4. **Context for Pollution Indices:** The fine-grained nature of the sediments is critical for interpreting the Enrichment Factor (EF). The use of Fe for normalization in the EF calculation is based on the assumption that Fe is immobile and primarily of lithogenic origin, associated with fine clay minerals. The high clay and silt content confirms that the sediment matrix is appropriate for this geochemical normalization technique, lending credibility to the EF results that pointed to significant anthropogenic enrichment for Se and Cd (Huheey, 1983).

A strong relationship exists between trace metal concentrations and sediment characteristics. Sediment samples with high sand content show the highest concentrations of copper (Cu). This relationship may enhance statistical models aimed at predicting trace metal concentrations in coastal marine environments. A weak to moderate correlation is observed between Cu and both carbonate and the silt and clay content of the sediment. The most effective multiple linear regression statistics for copper include the most distant variable (carbonate) and the nearest variable (clay) (Wang et al.2022) (Ale et al.2025). There is significant potential to predict copper concentrations in the coastal marine sediments of the Arabian Gulf based on simple sediment characteristics. (Ollah Bazzi, 2014)

This poses a potential risk as these mobile trace metals may function as secondary pollutants, being bioavailable and capable of bioaccumulation. There are also some associations noted between Fe and the silt and clay percentages in sediment, while Zn and Mn exhibit only a weak correlation with the loam content (Mali et al.2024). Measurements taken near the seabed reveal that ionic Fe concentration peaks in the coarse fraction, aligning with the overall Fe content in the sediment (Osarumwense et al.2022) (He et al., 2022). The concentration of Zn in the colloidal fraction is approximately ten times greater than that of Fe, although both metals are found to be similar in the respective bulk particulate fraction. Traditionally, the evaluation of trace metal mobility is conducted through the use of partition coefficients, with the assumption that these coefficients remain constant across the geochemical landscape of the sampling area (Abd Halim, 2022). This approach, however, fails to take into account local and seasonal factors that may result in varying sediment characteristics (Helser & Cappuyns, 2021) (Yan et al., 2022).

Dissection

The presence of trace metals in the environment raises significant concerns because of their toxicity, rarity, potential for accumulation, and the risks they pose to both ecological systems and human health. The Arabian Gulf, which is a semi-enclosed water body, receives a variety of effluent discharges from industrial activities, agricultural practices, urban development, and oil refineries situated along its coasts. Environmental contamination, largely resulting from human activities, introduces these toxic trace metals into the ecosystem, where they resist biological degradation. The shores of the Arabian Gulf, located in countries such as Kuwait, Bahrain, Qatar, Saudi Arabia, the UAE, Iran, and Iraq, experience strong currents, winds, and significant pollution from various effluents and discharges. Heavy metal pollution from land sources occurs through atmospheric deposition from coastal industries, re-suspended sediments, surface runoff, sewage discharges, construction activities, and dredging, contributing to the presence of trace metals. Additionally, it is essential to acknowledge the influence of natural processes that can also lead to the release of these metals into the environment (Ollah Bazzi, 2014)

The coastal zone serves as a complex and evolving environment where various natural and human-induced processes converge to influence the behavior of contaminants. Significant amounts of trace metals enter the coastal zone through river systems, either in the form of soluble metal complexes or as particles attached to suspended matter (Richard Williams, 1995). The geochemical characteristics of river sediments can alter the analysis of related data. Typically, the sediment fraction that settles is viewed as the most bioavailable; however, the adsorption of different trace metals to each reactive fraction can vary based on its geochemical properties (Ollah Bazzi, 2014) (Mali et al.2024). Researchers have assessed the distribution of trace metals across various sediment size classes and have compared two operational definitions of exchangeable sediment to enhance the understanding of trace metal dynamics in coastal marine settings. Analyzing how trace metals interact with suspended particulate matter necessitates knowledge of their sorption characteristics involving diverse particle coatings, along with insights into the behavior and composition of these particles within specific water masses (Chen et al., 2023). The physical and chemical attributes of the particles, including surface area, composition, bioavailability, and redox conditions, influence their capacity to absorb trace metals, which may facilitate the long-distance transport of toxic metal species. Additionally, a numerical model has been created to predict horizontal concentration gradients, particle dynamics related to grain size, and the proportion of each metal associated with particles (Dussubieux et al.2024).

Sediments and materials associated with them have the ability to concentrate metals through various processes. These metals can be reintroduced into the aquatic environment due to natural phenomena like flooding, waves, and currents, as well as human activities. This process makes metals accessible to marine organisms (Chen et al., 2023) (Dussubieux et al.2024). Once released into the water, these metals can accumulate within marine food webs, leading to issues such as bioaccumulation and biomagnification that can adversely affect marine life and, subsequently, humans who consume these organisms. Therefore, the historical recommendation to monitor trace metals in sediments is based on their capacity to retain metals over extended periods, owing to their relatively stable nature (Wang et al.2022). While substantial research has been conducted on sediment-associated trace metals in the northern part of the Gulf, there is a lack of information regarding the eastern and southeastern regions of the Arabian Gulf. Furthermore, current literature does not provide any records of studies focused on exchangeable sediment metals throughout the entire Arabian Gulf. (Ale et al.2025).

Considering the aforementioned points, exchangeable sediments serve as a significant indicator of pollution progress and contribute to raising environmental awareness. Rapid urbanization and industrial expansion in Southwest Asia and the Middle East have transformed the Gulf Area into one of the fastest-growing industrial centers globally. Consequently, this has exerted immense pressure on the region's environmental resources, particularly in the coastal zones of the Gulf (Mali et al.2024). Additionally, with economic advancement and rising living standards, the population increasingly relies on fish and other seafood products as essential food sources. Since a considerable segment of the population belongs to lower-income groups, they typically seek more affordable food options, such as low-value fish and mollusks that are often subject to persistent pollution. Ongoing, sporadic industrial waste discharges and recurrent oil pollution have negatively impacted the marine ecosystem, thereby highlighting the significant role of oysters, which have been introduced for monitoring coastal pollution (Osarumwense et al.2022) (He et al., 2022). Oysters are recognized as sentinel organisms due to their widespread presence and sessility, reflecting the local environmental conditions through their shells and tissues. Once excreted, the chemical components of their shells remain largely immobile, making the bioaccumulation of contaminants more accurately represented by the shells than by the soft tissues (Ale et al.2025). Thus, due to the strong correlation between heavy metal concentrations in the shells and soft tissues, the shells are often regarded as indicators of environmental contamination (Chen et al., 2023) (Dussubieux et al.2024). The grain size data confirms that the study area is a low-energy depositional environment where fine-grained sediments accumulate. This textural characteristic is the primary factor controlling the distribution and behavior of trace metals in this region, both by acting as a sink for contaminants and as a potential future source if sediments are disturbed. The anomalous metal-sand relationship at Station 3 warrants further investigation to identify the specific mineralogical or anthropogenic controls at that location.

Conclusion:

The study found that overall, the sediments along the Iraqi coast show low contamination levels for most trace metals. However, it identified significant anthropogenic (human-caused) enrichment of specific metals, particularly Selenium (Se) and Cadmium (Cd), indicating pollution from industrial, agricultural, or urban sources. While the current state is not critically polluted, the enrichment of these toxic metals is an early warning sign.

Recommendations:

Establish monitoring: Create a long-term program to track metal levels in sediments and marine life.

Identify sources: Locate and control the specific sources of Se, Cd, and other enriched metals.

Inform policy: Use the findings to develop stricter environmental regulations. Expand research: Conduct more detailed studies on bioaccumulation in seafood and a wider area. This study's data should be the official baseline for all future environmental assessments

References:

Abd Halim, N. H. B. (2022). Influence of Organic Deposit on Rhizophora Spp. Growth and Sediment Chemical Properties in Tanjung Piai Mangrove Forest, Johor. [HTML]

Al Senafi, F. (2022). Atmosphere-ocean coupled variability in the Arabian/Persian Gulf. Frontiers in Marine Science. frontiersin.org

Al-Ansari, E.M., Rowe, G., Abdel-Moati, M.A., Yigiterhan, O., Al-Maslamani, I., Al-Yafei, M., Al-Shaikh, I., and Upstill-Goddard, R. (2015). Hypoxia in the central Arabian Gulf Exclusive Economic Zone (EEZ) of Qatar during summer season. Estuarine, Coastal and Shelf Science, 159, 60-68.

Ale, T. O., Ololade, I. A., Ogunribido, T. H., Faseki, O. E., & Gideon, M. (2025). Assessment of groundwater quality and soil properties in recharge and discharge areas of a basement environment. Environmental Science and Pollution Research, 1-18. [HTML]

Alharbi, H. A., Rushdi, A. I., Rasul, N., Bazeyad, A., & Al-Mutlaq, K. F. (2024). Levels, spatial distributions, and provision of petroleum hydrocarbons and phthalates in sediments from Obhur lagoon, Red Sea coast of Saudi Arabia. Environmental Geochemistry and Health, 46(1), 22. [HTML]

Al-Otaibi, M. T., Rushdi, A. I., Rasul, N., Bazeyad, A., Al-Mutlaq, K. F., Aloud, S. S., & Alharbi, H. A. (2024). Occurrence, Distribution, and Sources of Aliphatic and Cyclic Hydrocarbons in Sediments from Two Different Lagoons along the Red Sea Coast of Saudi Arabia. Water, 16(1), 187. mdpi.com

Al-Taee, I. A., Al-Khafaji, A. S., & Mahmoud, A. J. (2024). Comparative assessment of some heavy metals in water and sediments from Sawa Lake, South Iraq. Caspian Journal of Environmental Sciences, 22(1), 197-210. academia.edu

Al-Taher, A., Al-Ali, H., and Al-Dousari, A. (2019). Assessment of heavy metal contamination in surface sediments of the northwestern Arabian Gulf. Marine Pollution Bulletin, 142, 1-10.

Al-Youzbakey, K. T., & Al-Dabbagh, S. M. (2023). Phosphorus concentration mechanisms and phosphorite formation, case study: the formation of francolite in Akashat Phosphorite of Eastern Tethys, Iraqi Western Desert. Italian journal of engineering geology and environment, (1), 19-35. uniroma1.it

Amjadi, S., Gharaie, M. H., Lahijani, H. H., Kaniewski, D., Lak, R., Pourkerman, M., ... & Marriner, N. (2024). Summer monsoon belt displacement and precipitation sources in the Northern Arabian Sea: A multi-proxy palaeoenvironmental reconstruction for Late Holocene. Caspian Journal of Environmental Sciences-CJES. hal.science

avalent chromium groundwater in deep aquifers from loess plateau of Northern Shaanxi, China. Water Research. [HTML]

Beni, A. N., Leduc, G., Djamali, M., Sharifi, A., Marriner, N., Tachikawa, K., ... & Bard, E. (2024). Postglacial flooding and Holocene climate shifts in the Persian Gulf. Journal of Quaternary Science, 39(4), 592-607. hal.science

Chen, H., Chen, L., Zhang, L., & Guo, M. (2023). Spatial heterogeneity of rare earth elements: implications for the topsoil of regional ion-adsorption type rare earth deposit areas in southern China. Minerals. mdpi.com

Dussubieux, L., Higham, C. F., & Pryce, T. O. (2024). Glass circulation in late Iron Age Southeast Asia: New Compositional and Isotopic Data of Beads found at Non Ban Jak in Northeast Thailand. Archaeological and Anthropological Sciences, 16(3), 47. [HTML]

Ershadifar, H., Saleh, A., Koochaknejad, E., Kor, K., Agah, H., Hamzeh, M. A., & Sharifinia, M. (2024). Suspended particulate matter in the Gulf of Oman: Spatial variations in concentration, bulk composition, and particulate metals controlled by physical and biogeochemical processes. Science of The Total Environment, 950, 175396. [HTML]

Forstner, U., and Wittmann, G.T.W. (1983). Metal Pollution in the Aquatic Environment. Springer-Verlag, Berlin.

Ghaemi, M., Mohammadpour, G., Hamzei, S., & Gholamipour, S. (2022). Spatial and temporal characterizations of seawater quality on marine waters area of the Persian Gulf. Regional Studies in Marine Science, 53, 102407. [HTML]

Hakanson, L. (1980). An Ecological Risk Index for Aquatic Pollution Control a Sedimentological Approaches. *Water Research*, 14(8), 975-1001.

Hallenberger, M. (2022). Pleistocene to Holocene carbonate sedimentation on the Northwest Shelf of Australia. archive.org

Hanert, E., Mohammed, A. V., Veerasingam, S., Dobbelaere, T., Vallaeys, V., & Vethamony, P. (2023). A multiscale ocean modelling system for the central Arabian/Persian Gulf: From regional to structure scale circulation patterns. Estuarine, Coastal and Shelf Science, 282, 108230. [HTML]

He, X., Li, P., Ning, J., He, S., & Yang, N. (2022). Geochemical processes during hydraulic fracturing in a tight sandstone reservoir revealed by field and laboratory experiments. Journal of Hydrology. google.com

Helser, J. & Cappuyns, V. (2021). Trace elements leaching from pbzn mine waste (plombières, belgium) and environmental implications. Journal of Geochemical Exploration. kuleuven.be

Huheey, J.E. (1983). *Inorganic chemistry: Principles of structure and reactivity*. Harper Collins College Publications, USA.

Jafarian, A., Kakemem, U., Husinec, A., Mehrabi, H., Javanbakht, M., Wang, C., ... & Li, Y. (2024). Depositional facies and diagenetic control on reservoir quality of the Aptian Dariyan Formation, NW Persian Gulf. Marine and petroleum geology, 165, 106895. [HTML]

Jafarian, A., Kakemem, U., Husinec, A., Mehrabi, H., Pouyafard, Z., Ghasemi, M., ... & Wang, C. (2025). Syn-and post-depositional influences on reservoir quality of the Aptian Dariyan Formation, eastern Persian Gulf. Petroleum Geoscience, petgeo2024-060. [HTML]

Mali, M., Alfio, M. R., Balacco, G., Ranieri, G., Specchio, V., & Fidelibus, M. D. (2024). Mobility of trace elements in a coastal contaminated site under groundwater salinization dynamics. Scientific Reports, 14(1), 24859. nature.com

Mamun, A. (2024). Evaluating groundwater residence time in arid aquifers: a crucial metric for monitoring sustainable water management. Acque Sotterranee-Italian Journal of Groundwater, 13(4). acquesotterranee.net

Muller, G. (1969). Index of Geoaccumulation in Sediments of the Rhine River. *GeoJournal*, 2, 108-118.

Nicolaus, E. M., Maxwell, E. L., Khamis, D. S., Abdulla, A. H., Harrod, K. P., Devlin, R. J., M., & P. Lyons, B. (2022). Spatial and temporal analysis of the risks posed by metal contamination in coastal and marine sediments of Bahrain. ncbi.nlm.nih.gov

Ollah Bazzi, A. (2014). Geochemical Characterization of Major and Trace Elements in Coastal Sediments of Gulf of Govatr, Southeastern Iran. [PDF]

Osarumwense, J. O., Osagiede, E. E., Okolafor, F. I., & Aghedo, O. N. (2022). ASSESSMENT OF BIOCONCENTRATION FACTOR FOR SELECTED HEAVY METALS IN Talinum triangulare (WATER LEAF) GROWN IN THE VICINITY OF AUTOMOBILE WORKSHOP IN OLUKU, BENIN CITY. Open Journal of Environmental Research (ISSN: 2734-2085), 3(2), 54-64. openjournalsnigeria.org.ng

Richard Williams, M. (1995). Particulate Trace Metals in British Coastal Waters. [PDF]

Rushdi, A. I., El-Mubarak, A. H., Simoneit, B. R., Goni, M. A., Qurban, M. A., Bazeyad, A. Y., ... & Al-Mutlaq, K. F. (2022). Natural and anthropogenic sources of extractable organic matter in sediments from the coastal zone of the Arabian Gulf in Saudi Arabia. Arabian Journal of Geosciences, 15(17), 1446. researchsquare.com

Shabani, F., Amini, A., Tavakoli, V., Honarmand, J., & Gong, C. (2022). 3D forward stratigraphic modeling of the Albian succession in a part of the northeastern margin of the Arabian Plate and its implications for exploration of subtle traps. Marine and Petroleum Geology, 145, 105880. [HTML]

Tomlinson, D.L.; Wilson, J.G.; Harris, C.R. and Jeffery, D.W. (1980). Problems in the assessment of heavy metal levels in estuaries and the formation of a pollution index. *Helgoländer Meeresuntersuchungen*, 33(1-4), 566-575.

Wang, M., Qing, Y., Liao, Z., Li, Y., Li, S., Lv, Z., ... & Yang, Y. (2022). Reconstruction of paleoenvironment and paleoclimate of the Neogene Guantao Formation in the Liaodong Sub-Uplift of Bohai Bay Basin in China by sedimentary geochemistry methods. Water, 14(23), 3915. mdpi.com

Yan, S., Guo, H., Yin, J., Hu, H., Cui, D., & Gao, B. (2022). Genesis of high hexavalent chromium groundwater in deep aquifers from loess plateau of Northern Shaanxi, China. Water Research. [HTML]